Variational study of the extended Hubbard-Holstein model on clusters of variable site spacing

Marcello Acquarone,[1] Mario Cuoco,[2] Canio Noce,[2] and Alfonso Romano[2]
[1]*CNR-GNSM, Unità I.N.F.M. di Parma, Dipartimento di Fisica dell'Università di Parma, I-43100 Parma, Italy*
[2]*Unità I.N.F.M. di Salerno, Dipartimento di Scienze Fisiche ''E.R. Caianiello,'' Università di Salerno, I-84081 Baronissi (Salerno), Italy*
(Received 3 August 2000; published 2 January 2001)

We study the complete extended Hubbard-Holstein Hamiltonian on a four-site chain with equally spaced sites, with spacing-dependent electronic interaction parameters evaluated in terms of Wannier functions built from Gaussian atomic orbitals. By successive application of generalized displacement and squeezing transformations, an effective polaronic Hamiltonian is obtained, containing a purely phonon-induced, long-range intersite charge interaction. The phase diagrams for $N=1$, 2, 3, and 4 electrons are determined by variational minimization of the sum of the electronic and the phononic energy, paying special attention to the effects of the above-mentioned phonon-induced long-range interaction. To characterize the physics of each ground state, we evaluate how variations of the site spacing affect the behavior of several correlation functions of experimental interest, with the aim of representing lattice deformation effects, either spontaneous or induced by external pressure.

DOI: 10.1103/PhysRevB.63.035110 PACS number(s): 71.27.+a, 71.38.−k, 63.20.Kr

I. INTRODUCTION

A model describing correlated electrons in a narrow band interacting locally with lattice deformations, the so-called Holstein-Hubbard model, was studied intensively in the last years both on infinite lattices[1–9] and on small clusters.[10–17] The classes of materials to which the model is assumed to apply, such as, for instance, high-temperature superconducting cuprates or the manganites showing colossal magnetoresistance, are characterized by rather strong electron-phonon coupling, so that a perturbative treatment is in general unreliable. In this case, one can apply to the interacting electron-phonon Hamiltonian a unitary ''displacement'' transformation[18] generated by a suitably chosen anti-Hermitian operator D. From the displaced Hamiltonian $\tilde{H}=e^{D}He^{-D}$, a nonperturbative effective Hamiltonian for phonon-dressed electrons (polarons) can be obtained by averaging $\tilde{H}$ over an appropriate phonon wave function. In recent years, the use of variationally optimized ''squeezed'' phonon states of the form $e^{-S}|0_{ph}\rangle$, with $|0_{ph}\rangle$ being the phonon vacuum, proved to be advantageous[3,9,11,19] over methods using simple harmonic-oscillator states. However, as the operators D and S on a lattice with L sites each contain L undetermined c numbers, one for each phonon wave vector q, such procedure requires to set all such $2L$ displacement and squeezing parameters to their optimal values. A variational determination on an infinite lattice is therefore impossible, and one has to adopt perturbative techniques.[20,21] For this reason, the most popular approach has been to neglect the q dependence of the displacement parameters, by assuming $\delta_q=1$ for any q. This is the standard Lang-Firsov approximation (LFA),[22] which, however, has at least two limitations. On the one hand, it neglects any intersite phonon correlation, preventing the study of how the charge on a given site can also induce deformations on different sites, possibly giving rise to extended polarons.[23] On the other hand, one can show[24] that, for nondispersive phonons, the LFA leads to a vanishing of a purely phonon-induced intersite charge interaction (the ''residual interaction'' first introduced in Ref. 25), in principle present in $\tilde{H}$. One concludes that the physics of the system is not faithfully represented in the LFA. If, instead of infinite lattices, one considers small clusters,[10] the numerical complexity is reduced, and one can rigorously take into account the q dependence of all the variational parameters. In this way the limitations of the LFA can be avoided, and, in particular, the intersite correlations between charges and deformations, as well as the effects of the purely phonon-induced interaction terms, can be satisfactorily taken into account.

This is actually one of the points on which the present work focuses. Indeed, we shall first derive the effective polaronic Hamiltonian from a bare Hamiltonian which, in the electronic part, includes all the one- and two-body interactions compatible with a nondegenerate band of electrons, and has an electron-phonon coupling of the Holstein type. As far as the set of electronic interactions is concerned, the present work extends previous studies, where the only two-body electronic coupling terms included in the bare Hamiltonian were the on-site and intersite Coulomb charge interactions. Then we shall exactly solve the effective model on a four-site chain with a constant intersite distance a and closed boundary conditions. Considering that in this case the wave vector q takes four values, given by $-\pi/2a$, 0, $\pi/2a$, and π/a, the independent displacement and squeezing parameters are six in total, as $\delta_{\pi/2a}=\delta_{-\pi/2a}$ and $\alpha_{\pi/2a}=\alpha_{-\pi/2a}$. They will be simultaneously and independently determined by an exact diagonalization of the effective Hamiltonian, followed by a variational optimization of the ground-state energy, for a given, but arbitrary, site spacing and a given shape of the Wannier functions, as discussed below. This will allow us, on the one hand, to discuss the interplay between charges and phonons both on the same site and on different sites, and, on the other hand, to properly take into account the effect of the phonon-induced intersite charge interaction.

Another aspect of the present work is that, as we model the dependence on the site spacing of all the electronic interaction parameters, we can study the phase diagram and correlation functions at any given filling as functions of the intersite distance. Our results can therefore give qualitative indications relevant both to measurements under mechanical or chemical pressure, and to materials showing ''stripes''[26] or other forms of spontaneously coupled charge and structural inhomogeneities,[27] where regions with different lattice parameters, and different electronic character, have been reported to coexist.

The paper is organized as follows. In Sec. II, we define the model and derive the effective polaronic Hamiltonian. The results of the numerical analysis on a four-site closed chain for different fillings $N=1$, 2, 3, and 4 are discussed in Sec. III. Sec. IV is devoted to conclusions.

II. MODEL AND THE EFFECTIVE HAMILTONIAN

Our model Hamiltonian $H=H_{el}+H_{el\text{-}ph}+H_{ph}$ consists of a generalized Hubbard Hamiltonian for correlated electrons coupled to phonons of frequency Ω_q. The bare electronic Hamiltonian reads

$$H_{el}=\sum_{j\sigma}\epsilon_j n_{j\sigma}-\sum_{jl\sigma}[t_{jl}-X_{jl}(n_{j,-\sigma}+n_{l,-\sigma})]c^{\dagger}_{j\sigma}c_{l\sigma}+U\sum_j n_{j\uparrow}n_{j\downarrow}+\sum_{jl}V_{jl}n_jn_l+\sum_{jl}J_{jl}\mathbf{S}_j\cdot\mathbf{S}_l+\sum_{jl}P_{jl}(c^{\dagger}_{j\uparrow}c^{\dagger}_{j\downarrow}c_{l\downarrow}c_{l\uparrow}+\text{H.c.}), \quad (1)$$

where $c^{\dagger}_{j\sigma}(c_{j\sigma})$ creates (annihilates) an electron with spin σ on site j, and $\mathbf{S}_j$ and n_j are the total spin and charge on site j, respectively. Following the procedure reported in Ref. 16, the bare electronic interactions ϵ, t, U, V, J, and X are parametrized by means of a Wannier function built from Gaussian functions $\phi_j(r)=(2\Gamma^2/\pi)^{3/4}\exp[-\Gamma^2(r-R_j)^2]$ modeling the atomic orbitals on the jth site in the position R_j. The Wannier functions, and by consequence the interactions, depend on the intersite distance a and the width Γ^{-1} of the orbitals. The explicit expressions of ϵ, t, U, V, J, P, and X that we use in this paper have been evaluated in the case of a dimer, and are given in Ref. 16. This allows us to estimate all the electronic parameters in an *ab initio* type scheme.

The interaction $H_{el\text{-}ph}$ between the electrons and the phonons is assumed to be of the Holstein type $H_{el\text{-}ph}=G\Sigma_{j\sigma}u_jn_{j\sigma}$, where u_j is the lattice deformation at site j. By introducing the characteristic length $\mathcal{L}_q=\sqrt{\hbar/2M\Omega_q}$ and the renormalized electron-phonon coupling $g_q\equiv G\mathcal{L}_q$, in second quantization $H_{el\text{-}ph}$ takes the form

$$H_{el\text{-}ph}=\sum_q g_q(b^{\dagger}_{-q}+b_q)n_q, \quad (2)$$

where $n_q=L^{-1/2}\Sigma_{j,\sigma}n_{j,\sigma}\exp[iqR_j]$, L being the number of lattice sites. Finally, the free-phonon term

$$H_{ph}=\sum_q \hbar\Omega_q(b^{\dagger}_qb_q+1/2) \quad (3)$$

completes the model Hamiltonian. The general procedure to obtain the effective polaronic Hamiltonian and to identify its ground state consists in the following steps.[16]

(i) A unitary transformation generated by a suitably chosen anti-Hermitian operator D is used to map the model Hamiltonian H onto the ''displaced'' Hamiltonian $\tilde{H}=e^{D}He^{-D}$.[18] We choose

$$D=\sum_q \delta_q\frac{g_q}{\hbar\Omega_q}(b^{+}_{-q}-b_q)n_q, \quad (4)$$

where the parameters δ_q, defined on the L wave vectors of the first Brillouin zone, measure the degree of ''displacement'' of the corresponding phonon mode. Their real-space expressions δ_{jl}, associated with the coupling between charge on site j and phonons on site l, are given by $\delta_{jl}=(1/L)\Sigma_q\delta_q\exp[iq(R_j-R_l)]$. It is evident that assuming $\delta_q=1$ for any q (as it is done in the LFA) implies that $\delta_{jl}=0$ if $R_j\neq R_l$, forcing the effective interactions to be strictly local.

(ii) By averaging $\tilde{H}$ over the squeezed phonon state $|\Psi_{ph}\rangle$,[19,28] the phononic degrees of freedom are eliminated, yielding an effective polaronic Hamiltonian. The squeezed state is defined as $|\Psi_{ph}\rangle=e^{-S}|0_{ph}\rangle$,[11,19,28] where $|0_{ph}\rangle$ is the harmonic-oscillator vacuum state, such that $b_q|0_{ph}\rangle=0$, and the squeezing generator S, expressed in terms of the L variational parameters α_q (or, in real space, $\alpha_{jl}=(1/L)\Sigma_q\alpha_q\exp[iq(R_j-R_l)]$), reads

$$S=\sum_q \alpha_q(b^{\dagger}_qb^{\dagger}_{-q}-b_qb_{-q})=\sum_{j,l}\alpha_{jl}(b^{\dagger}_jb^{\dagger}_l-b_jb_l). \quad (5)$$

This procedure leads to an effective Hamiltonian H^* describing phonon-dressed electrons (which we shall generally designate as polarons) having the form

$$H^*=\sum_q\hbar\Omega_q\left[\sinh^2(\alpha_p)+\frac{1}{2}\right]+\sum_{j\sigma}\epsilon^*_jn_{j\sigma}-\sum_{jl\sigma}[t^*_{jl}-X^*_{jl}(n_{j,-\sigma}+n_{l,-\sigma})]c^{\dagger}_{j\sigma}c_{l\sigma}+U^*\sum_j n_{j\uparrow}n_{j\downarrow}+\sum_{jl}V^*_{jl}n_jn_l+\sum_{jl}J^*_{jl}\mathbf{S}_j\cdot\mathbf{S}_l+\sum_{jl}P^*_{jl}(c^{\dagger}_{j\uparrow}c^{\dagger}_{j\downarrow}c_{l\downarrow}c_{l\uparrow}+\text{H.c.}), \quad (6)$$

with the renormalized interactions

$$\epsilon^*_j=\epsilon_j-\frac{1}{L}\sum_q\frac{g^2_q}{\hbar\Omega_q}\delta_q(2-\delta_q), \quad (7)$$

$$U^*_j=U_j-2\left(\frac{1}{L}\right)\sum_q\frac{g^2_q}{\hbar\Omega_q}\delta_q(2-\delta_q), \quad (8)$$

$$V_{jl}^{*}=V_{jl}-\frac{1}{L}\sum_{q}\frac{g_q^2}{\hbar\Omega_q}\delta_q(2-\delta_q)e^{iq(R_j-R_l)}, \tag{9}$$

$$t_{jl}^{*}=\tau t_{jl},\quad X_{jl}^{*}=\tau X_{jl},\quad P_{jl}^{*}=\tau^4 P_{jl},\quad J_{jl}^{*}=J_{jl} \tag{10}$$

$$\tau=\exp\left\{-\frac{1}{L}\sum_{q}\left(\frac{g_q}{\hbar\Omega_q}\right)^2\delta_q^2[1-\cos(qa)]e^{-2\alpha_q}\right\}. \tag{11}$$

(iii) The eigenstates and eigenvalues of the polaronic Hamiltonian are determined by using an exact diagonalization method proposed in Ref. 29.

(iv) The optimal values of the displacement and squeezing parameters are determined variationally by minimizing the total energy of the electron-phonon system.

A detailed derivation of Eqs. (7)–(11) is given in Ref. 24. We see that all the parameters but J are renormalized to some extent by the phonons. The one- and two-particle hopping amplitudes (t_{jl}^{*}, X_{jl}^{*}, and P_{jl}^{*}, respectively) depend on the hopping reduction factor τ, whose value, once the optimal δ_q and α_q are given, follows from Eq. (11). The charge mobility is thus controlled simultaneously, and competitively, by the displacement and the squeezing parameters.

In the following, all the bare intersite coupling constants will be assumed to be nonvanishing only between nearest-neighbor sites. We stress that, even under this assumption, the effective intersite density-density interaction V_{jl}^{*} [Eq. (9)] acquires a phonon-dependent long-range contribution generally extending beyond nearest-neighbor sites. If dispersionless phonons of frequency Ω are assumed, then this phonon-induced long-range part of the Coulomb interaction remains nonvanishing only if the q dependence of the displacement parameters is explicitly accounted for. This interaction was first discussed within the LFA, for dispersive phonons, in Ref. 25, but with no attempt of estimating its value. A more recent variational study,[5] employing a nonfactorized fermion-boson wave function in the context of a simple Hubbard electronic Hamiltonian (i.e., such that $X_{ij}=V_{ij}=J_{ij}=P_{ij}=0$), also found an analogous effective interaction.

III. RESULTS

The general procedure illustrated in Sec. II has been applied to the case of a four-site chain with dispersionless phonons of frequency $\hbar\Omega=0.1$ eV, a value appropriate to cuprates and manganites. The eigenvalues and eigenvectors of the effective Hamiltonian have been exactly calculated using the method outlined in Ref. 29. The knowledge of all the eigenvalues for given a and Γ allows one to identify the ground state by the independent and simultaneous optimization of the wave-vector-dependent variational parameters defining, for each phonon mode q, the degree of displacement (δ_q) and squeezing (α_q). Once the optimal values of the parameters are identified, the full eigenvalue spectrum can be obtained. The value of Γ might also have been obtained variationally, as in Ref. 16,[35] but due to the increased complexity of the numerical analysis we have investigated the phase diagram only for three representative values of Γ, equal to 0.8, 1, and 1.2 Å^{-1}. We find that Γ^{-1} roughly scales as a in determining the main features of the phase diagram. The differences in the phase diagram for different Γ values at given N are only quantitative, and correspond to slight variations of the border lines between the different phases. In particular, we have found that for increasing N the effects induced by variations of Γ tend to become less and less significant. Therefore, we will limit ourselves to the discussion of the results obtained in the case $\Gamma=1$ Å^{-1}. A study of the half-filled case for fixed a and varying Γ was already published.[30]

Given the operators A_i and B_j, defined at sites i and j, we evaluate the correlation function (CF) $\langle A_iB_j\rangle$ in the ground state $|G\rangle$ of the effective Hamiltonian H^{*} according to

$$\langle A_iB_j\rangle=\langle G|\langle 0_{ph}|e^{S}e^{D}A_iB_je^{-D}e^{-S}|0_{ph}\rangle|G\rangle. \tag{12}$$

The nature of the ground state is investigated for different fillings by evaluating the dependence on the lattice constant of the spin and charge CF's,

$$\chi_n^{s}=\frac{1}{L}\sum_{i}\langle \mathbf{S}_i\cdot\mathbf{S}_{i+1}\rangle, \tag{13}$$

$$\chi_{nn}^{s}=\frac{1}{L}\sum_{i}\langle \mathbf{S}_i\cdot\mathbf{S}_{i+2}\rangle, \tag{14}$$

$$\chi_n^{c}=\frac{1}{L}\sum_{i}\langle n_in_{i+1}\rangle, \tag{15}$$

$$\chi_{nn}^{c}=\frac{1}{L}\sum_{i}\langle n_in_{i+2}\rangle, \tag{16}$$

with $\chi_n^{s,c}$ and $\chi_{nn}^{s,c}$ indicating the nearest and next-nearest neighbor CF's for the spin (s) and charge (c) channels, respectively. In addition, we have analyzed the behavior of the on-site, nearest- and next-nearest neighbor charge-deformation CF's, given by

$$\Phi_{loc}=\frac{1}{L}\sum_{j}\langle n_j(b_j^{\dagger}+b_j)\rangle, \tag{17}$$

$$\Phi_{a}=\frac{1}{L}\sum_{j}\langle n_j(b_{j\pm a}^{\dagger}+b_{j\pm a})\rangle, \tag{18}$$

$$\Phi_{2a}=\frac{1}{L}\sum_{j}\langle n_j(b_{j\pm 2a}^{\dagger}+b_{j\pm 2a})\rangle, \tag{19}$$

respectively. It is easy to show that the above charge-deformation CF's can be expressed as weighted sums of the charge CF's, with the real-space displacement parameters acting as weights. In the case of dispersionless phonons their expressions are

$$\phi_{loc}=\frac{g}{2\hbar\Omega}(n\,\delta_{loc}+2\,\delta_a\chi_n^{c}+\delta_{2a}\chi_{nn}^{c}), \tag{20}$$

$$\phi_a = \frac{g}{2\hbar\Omega}[(\delta_{loc}+\delta_{2a})\chi_n^c + \delta_a\chi_{nn}^c + n\delta_a], \tag{21}$$

$$\phi_{2a} = \frac{g}{2\hbar\Omega}(2\delta_a\chi_n^c + \delta_{loc}\chi_{nn}^c + n\delta_{2a}), \tag{22}$$

where $n=N/L$ is the electron density, and δ_{loc}, δ_a, and δ_{2a} are real-space displacement parameters, associated with the coupling of an electron to a lattice distortion on the same site, on the nearest-neighbor site, and on the next-nearest neighbor site. Recalling that for a four-site chain the wave vector q takes the four values $-\pi/2a$, 0, $\pi/2a$, and π/a, and assuming $\delta_{-\pi/2a}=\delta_{\pi/2a}$ and $\alpha_{-\pi/2a}=\alpha_{\pi/2a}$, one obtains that the expressions of δ_{loc}, δ_a, and δ_{2a} in terms of the q-dependent displacement parameters are

$$\delta_{loc} \equiv \delta_{ii} = \tfrac{1}{4}(\delta_0 + 2\delta_{\pi/2a} + \delta_{\pi/a}), \tag{23}$$

$$\delta_a \equiv \delta_{i,i+1} = \tfrac{1}{4}(\delta_0 - \delta_{\pi/a}), \tag{24}$$

$$\delta_{2a} \equiv \delta_{i,i+2} = \tfrac{1}{4}(\delta_0 - 2\delta_{\pi/2a} + \delta_{\pi/a}) \tag{25}$$

(similar expressions are obtained for the real-space squeezing parameters α_{ij}). It is worth noting that in the case of a single electron (i.e., $N=1$), Eqs. (20)–(22) give a simple relation of proportionality between the functions Φ and the parameters δ evaluated at the same site distance.

In the numerical analysis for $N\geqslant 2$ we paid special attention to the effect on the phase diagram of the phonon-induced charge interaction, by distinguishing the results obtained by including both nearest ($V^*_{i,i\pm1}$) and next-nearest ($V^*_{i,i\pm2}$) intersite charge interactions, from those obtained for $V^*_{i,i\pm2}=0$. The behavior of the correlation functions and the renormalized electronic interactions, discussed in the next sections, always refer to the cases of $V^*_{i,i\pm1}$ and $V^*_{i,i\pm2}$, both nonvanishing, with the parameter Γ chosen equal to 1 Å^{-1}. We have also verified that at any filling the parameters X^*, P^*, and $J^*=J$ are very small, and have no influence on the phase diagram. Therefore, their behavior will not be shown in the following. We shall analyze the results for the fillings $N=1$, 2, 3, and 4 separately.

A. The Case $N=1$

We treat this case mainly to test the reliability of our approach as compared with other methods developed in the literature.[1,5–7,12,17,25] The phase diagram for $N=1$ is shown in Fig. 1.

The boundary separates two regions. In the lower one the polaron has a nonvanishing hopping amplitude, with the deformation involving, though very weakly, the first- and second-neighbor sites. In the upper region t^* vanishes together with Φ_a and Φ_{2a}, so that the polaron is trapped and the deformation is strictly local. This picture is in substantial agreement with the results presented in Refs. 7 and 12.

B. $N=2$, quarter-filling case

The phase diagram concerning the quarter-filling case ($N=2$) is plotted in Fig. 2 for $\Gamma=1$ Å^{-1} comparing the cases with and without $V^*_{i,i\pm2}$. We can distinguish three main regions: a disordered (D) phase without magnetization, a phase in which the two electrons behave as separated polarons (SP) in a superposition of configurations of the 1-0-1-0 type, and a phase characterized by the formation of an on-site bipolaron (OSB), i.e., a superposition of configurations of the 2-0-0-0 type.

We see that in this case the Coulomb interaction between next-nearest-neighbor sites $V^*_{i,i\pm2}$ affects the phase diagram rather strongly. Indeed, while there is no significant effect on the boundary of the OSB region, the inclusion of the effect

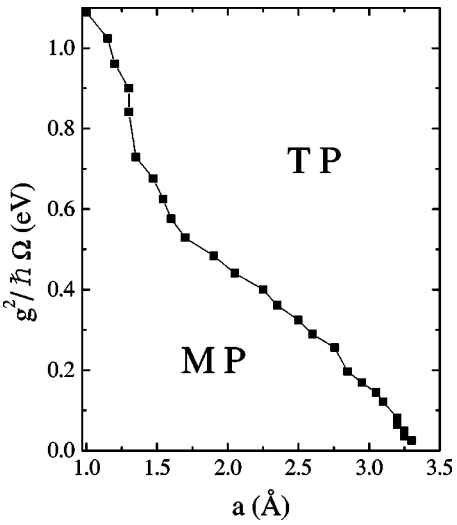

FIG. 1. Phase diagram for $N=1$ and $\Gamma=1$ Å^{-1}. The labels MP and TP stand for a mobile polaron and a trapped polaron, respectively.

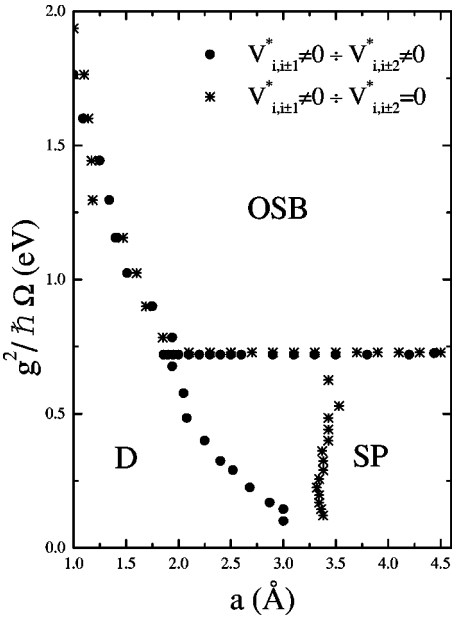

FIG. 2. Phase diagram for $N=2$ and $\Gamma=1$ Å^{-1}. The regions labeled D, SP, and OSB are characterized by the presence of charge and spin disorder, separated polarons, and on-site bipolarons, respectively.

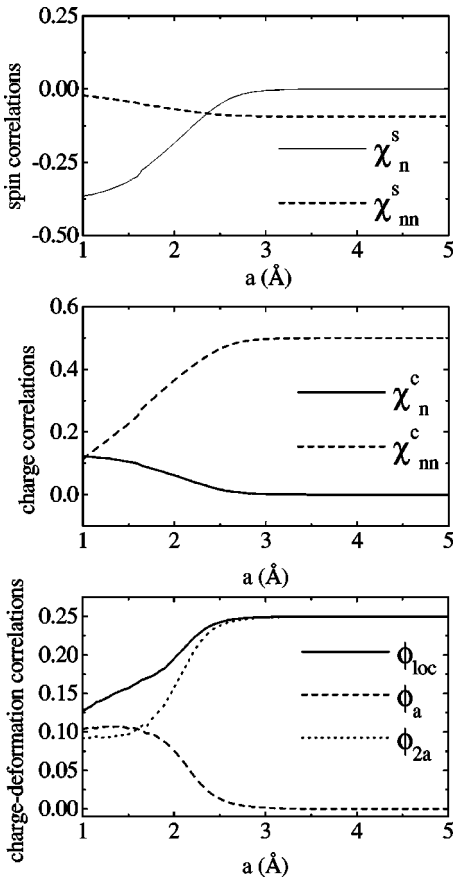

FIG. 3. Spin (top panel), charge (middle panel), and charge-deformation (bottom panel) correlation functions for $N=2$ at $g^2/\hbar\Omega=0.1$ eV.

of $V^*_{i,i\pm2}$ leads to a considerable enlargement of the D region at the expenses of the SP region, additionally changing the D-SP transition from sharp to smooth.

Let us discuss in more detail the D-SP crossover for a small polaron binding energy, choosing $g^2/\hbar\Omega=0.1$ eV. As one can see from Fig. 3 (top panel), the behavior of the spin CF's reveals a competition between different spin configurations in the ground state, without a clear predominance of one of them. In particular χ^s_{nn} is almost zero, while χ^s_n is negative in the D region, revealing a tendency toward an antiferromagnetic (AF) configuration. On the other hand, the charge CF's in the middle panel of Fig. 3 show that above a critical value of a (in the case considered in the figure, equal approximately to 2.8 Å), the charge distribution changes, giving rise to a pattern 1-0-1-0 of alternating singly occupied and empty sites which is characteristic of what we have called the SP region.

On the contrary, in the D region, χ^c_n and χ^c_{nn} are smoothly changing with a, revealing the presence of a fluctuating regime with disordered charge distribution. Let us stress that in the SP configuration there is no predominant character of either ferromagnetic or AF correlations, since the slightly negative values of χ^s_{nn} cannot be considered as a sign of the onset of an antiferromagnetic order. The displacement parameters and the charge-displacement correlation functions reveal additional interesting details of the transition.

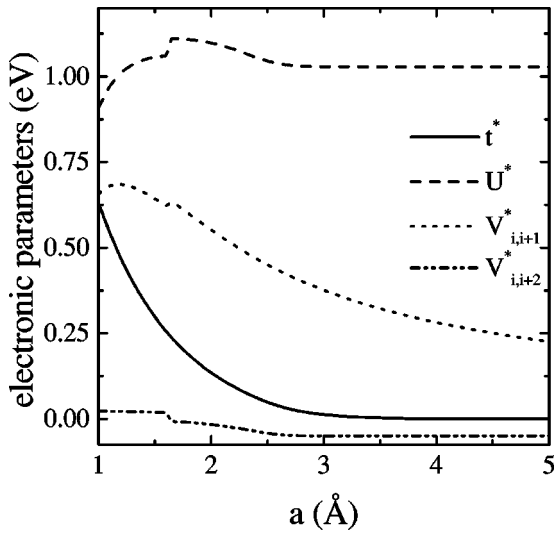

FIG. 4. Renormalized electronic interaction parameters for $N=2$ and $g^2/\hbar\Omega=0.1$ eV.

Actually, the bottom panel of Fig. 3 shows that there is a smooth, yet pronounced, change in the phononic regime for a approximately greater than 2 Å, thus well inside the D region. Indeed, for small values of a, all the charge-deformation CF's are non-negligible and comparable. Then, when a is increased above 2 Å, Φ_{loc} and Φ_{2a} grow, both converging to the value 0.25, while Φ_a decreases becoming negligible above $a=3$ Å. The resulting smooth crossover from the D phase to the SP phase shows that already in the D phase there are precursory effects of the charge ordering of the 1-0-1-0 type that characterizes the SP phase, stable at higher values of the intersite distance.

The corresponding behavior of the effective two-body parameters is shown in Fig. 4. In particular, it is interesting to note that a signature of the two phononic regimes in the D phase discussed above is clearly visible in the behavior of the next-nearest-neighbor interaction $V^*_{i,i\pm2}$, which already at $a\simeq1.7$ Å turns from repulsive to attractive, while both U^* and $V^*_{i,i\pm1}$ remain repulsive. This situation clearly promotes the SP type of charge order, which, however, can be stable only when the effective hopping amplitude t^* becomes negligible. It is worth pointing out that the D and SP states are very close in energy, so that even a small interaction like $V_{i,i\pm2}$ can significantly influence the position of the phase boundary.

Considering values of the polaron binding energy $g^2/\hbar\Omega$ greater than approximately 0.7 eV, we have that the increase of a induces a transition from the disordered phase to a new charge ordered phase, in which the local effective interaction U^* becomes strongly attractive, thus leading to the formation of an on-site localized bipolaron. The nature of the OSB region and the driving mechanism leading to its formation are clarified by the behavior of the renormalized electronic parameters. As one can see from Fig. 5, in the OSB phase the on-site Coulomb interaction is so strongly renormalized that it becomes attractive, while at the same time the kinetic energy vanishes. These behaviors of U^* and t^* lead to the formation of a localized on-site bipolaron.

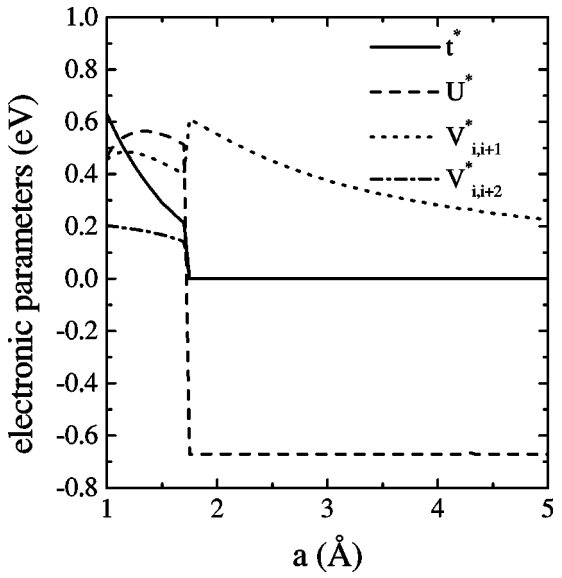

FIG. 5. Renormalized electronic interaction parameters for $N=2$ at $g^2/\hbar\Omega=0.9$ eV.

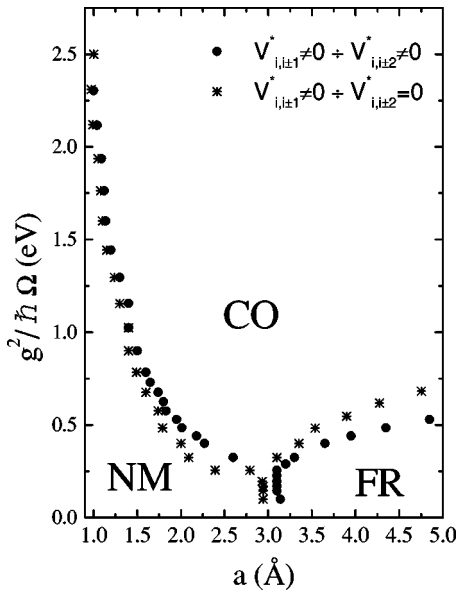

FIG. 6. Phase diagram for $N=3$ and $\Gamma=1$ Å^{-1}. The regions labeled NM, CO, and FR are characterized by vanishing magnetization, charge order, and frustrated magnetic order, respectively.

We have also found that in the OSB phase both χ^s_n and χ^s_{nn} vanish for any a, so that the phase is characterized by the absence of both spin correlations and local moments. In addition, the charge correlation functions χ^c_n and χ^c_{nn} are also identically vanishing, while Φ_{loc} is the only charge-deformation CF which is different from zero. These results clearly indicate that in the OSB phase the charge, together with its accompanying deformation, is completely localized on one of the chain sites, in a superposition of configurations of the 2-0-0-0 type. This was also verified by checking that in the ground-state wave function all the components of the 1-1-0-0 type have negligibly small amplitudes.

It is interesting to compare the present results with other studies on the behavior of two fermions coupled to lattice deformations. The main issue discussed in the literature is to clarify under which conditions a bound state of two polarons, i.e., a bipolaron, either on-site or intersite, is stable, and possibly itinerant. In the large $g^2/\hbar\Omega$ region, dominated by the negative value of U^*, our result of an essentially localized on-site bipolaron agrees with those in the literature.[12] We have also verified that, even imposing the vanishing of the bare intersite charge repulsion V_{ij}, the OSB region is not changed.

In the low $g^2/\hbar\Omega$ region, we do not find mobile intersite bipolarons, at variance with other studies.[5,6,8,12,13,17,31] In assessing the stability of either type of bipolaron, it is very important to take into account the bare contribution $V_{i,i\pm1}$ to the effective intersite charge interaction V^*_{ij}. In papers in which a stable intersite bipolaron was found, this term, that is repulsive and usually rather large (a sizeable fraction of U), was however neglected,[5,8,12,13,17] or explicitly assumed to be renormalized to an overall attractive value.[6] Another recent paper[31] emphasized the physical relevance of the intersite bipolarons. Within its LFA treatment of the long-range Fröhlich electron-phonon interaction with dispersive phonons, the bare V_{ij} is included, but the equivalent of our V^*_{ij} is estimated, on a purely phenomenological basis, to be very small, even between nearest neighbors.

Our main conclusion about the formation of a bipolaron and, in particular, on its size, is that, when the complete set of bare two-particle interactions is taken into account, for $N=2$ only on-site bipolarons are possible, this taking place in the range of parameters corresponding to the OSB region of Fig. 2. When stable, the OSB has a localized character, due to the simultaneous vanishing of the effective single-particle hopping t^* and the effective pair hopping amplitude P^*. Hence our results do not support the presence of intersite mobile bipolarons for realistic values of the interactions, even if, on the other hand, they cannot definitely be ruled out in infinite lattices.

Besides the limitations of dealing with a cluster, one might also question the approach that we adopt here to evaluate V_{ij},[16] yielding rather high values of the bare intersite repulsion that, for physically reasonable values of the phonon frequency Ω and the coupling strength g, can be only partially compensated for by the phonon renormalization. However, even if the absolute magnitudes of the various interactions we evaluate are model dependent, their ratios should be of more general applicability. Indeed, it is known that in several classes of physical systems the nearest-neighbor Coulomb interaction is a significant fraction of the on-site one. This is, for instance, the case of the high-T_c superconducting copper oxides, where theoretical estimates of $V_{i,i+1}$ (Refs. 4 and 32), give a repulsive value of the order of 0.2 eV.

C. $N=3$, one-hole case

The phase diagram for $N=3$ is shown in Fig. 6. We start by discussing phases that are stable at low values of the polaron binding energy, looking at the behavior of the correlation functions for $g^2/\hbar\Omega=0.1$ eV.

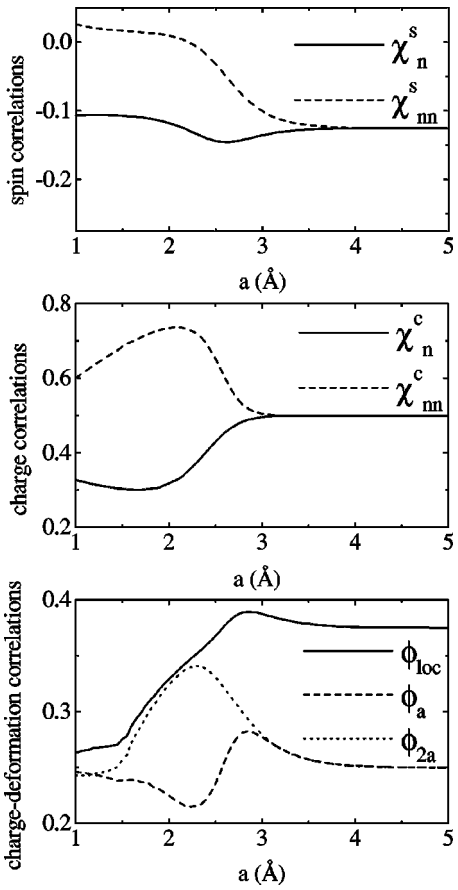

FIG. 7. Spin (top panel), charge (middle panel), and charge-deformation (bottom panel) correlation functions for $N=3$ at $g^2/\hbar\Omega=0.1$ eV.

As one can see from the upper panel of Fig. 7, the behavior of χ^s_n shows little change as a is varied, and is always negative. On the other hand, χ^s_{nn} is positive and close to zero for a smaller than $\simeq 2$ Å, and then it changes sign as a is increased, going to a saturation value of about -0.125. As far as the charge channel is concerned, we see from the middle panel of Fig. 7 that χ^c_n exhibits slight variations with a, with a smooth increase concentrated in a range going approximately from 2 to 3 Å. On the other hand, up to $a \approx 3$ Å χ^c_{nn} is larger than χ^c_n, first growing (up to $a \approx 2$ Å) and then smoothly decreasing toward the saturation value 0.5 that both χ^c_n and χ^c_{nn} reach for $a>3$ Å.

As far as the charge-deformation CF's are concerned, we see from the bottom panel of Fig. 7 that Φ_{loc} is the largest at any a, with Φ_{2a} manifesting a significant increase exactly in the range of intermediate values of a in which χ^c_{nn} reach its maximum. In addition Φ_a turns out to be the smallest charge-deformation CF at any a, becoming equal to Φ_{2a} only above $a \approx 3$ Å.

Combining the results for the CF's, we conclude that for a lower than ≈ 2 Å in the nonmagnetic (NM) region, the charge is distributed with fluctuating configurations of almost empty and almost doubly occupied next-nearest-neighbor sites. This causes both χ^c_{nn} and χ^s_{nn} to be negligible. Then, as a is increased beyond 2 Å up to $a \approx 3$ Å, there is, consistently with the behavior of Φ_{2a}, a crossover region which can be seen as a precursor of the charge order of 2-0-1-0 type, which characterizes the ground state of the system at higher values of $g^2/\hbar\Omega$. Finally, the charge distribution tends to become uniform as the system, for $a>3$ Å, enters the region that we label as ''frustrated magnetism'' (FR). Indeed, there χ^s_n and χ^s_{nn} converge to the same unsaturated negative value, which expresses a tendency of the spins to align antiferromagnetically both on nearest- and next-nearest-neighbor sites. The FR zone is also characterized by a reduction in the extent of the deformation around each occupied site, as indicated by Φ_{2a} becoming the smallest charge-deformation CF.

The renormalized electronic parameters (not shown) vary smoothly with a. They never change sign, with the exception of the long-range charge interaction which, always very small, changes from positive to negative near the NM-FR boundary.

Let us now consider larger values of the polaron binding energy, investigating in particular that part of the phase diagram, corresponding to values of $g^2/\hbar\Omega$ between approximately 0.25 and 0.7 Å, where a charge ordered (CO) phase develops between the NM and the FR regions for intermediate values of a. This will be done with a special attention to the character of the CO phase, by analyzing the behavior of the CF's at the representative value $g^2/\hbar\Omega=0.4$ eV. As one can see from the upper panel of Fig. 8, for values of a falling in a range going approximately from 2.2 to 3.7 Å, the spin CF's χ^s_n and χ^s_{nn} are zero, indicating the absence of local moments and magnetic correlations in the ground state. On the other hand, by looking at the behaviors of χ^c_n and χ^c_{nn} in the same range of values of a, we can see that charge correlations are vanishing on nearest-neighbor sites and tend to the maximum value compatible with the filling on next-nearest-neighbor sites. This is a clear indication of the development of an ordered configuration where the charge is fully distributed on next-nearest-neighbor sites.

The same general trend can be inferred from the charge-deformation CF's, shown in the lower panel of Fig. 8. We see that correlations between the charge and the deformations in the CO region become strongest between second-neighbor sites, with the first-neighbor one being the smallest. This can be interpreted as a further indication that the ground state is given by a superposition of the charge configurations 1-0-2-0 and 2-0-1-0, together with the symmetrically related 0-1-0-2 and 0-2-0-1 configurations. This degeneracy of the ground state, related to the fact that we cannot have a truly broken-symmetry state in finite-size systems, is also the reason why in the CO region χ^c_{nn} is equal to 1, rather than being equal to 2. The whole picture is also consistent with the behavior of the renormalized electronic parameters, featuring a non-negligible negative value of $V^*_{i,i\pm 2}$ both in CO and in FR regions.

The filling $N=3$ can be viewed as the case of one hole in a half-filled configuration. There are two different predictions on the related ground state in the limit of large U^*/t^*. According to Nagaoka's theorem, a ferromagnetic (FM) state should set in when $U\rightarrow\infty$ with t remaining finite, while,

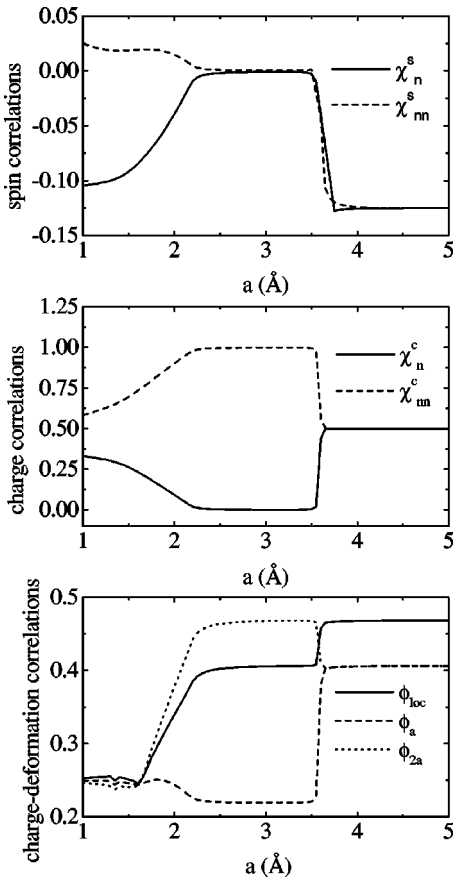

FIG. 8. Spin (top panel), charge (middle panel), and charge-deformation (bottom panel) correlation functions for $N=3$ at $g^2/\hbar\Omega=0.4$ eV.

according to Refs. 2, 6, 13, and 15, the hole would be a polaron in an antiferromagnetic background, where its phonon-induced localization would take place at a lower value of $g^2/\hbar\Omega$ due to concurrent effect of the ordered spin arrangement. In our approach we find that for $N=3$ none of the two magnetic ground states mentioned above is stable. Conversely, in what we have called the frustrated region no magnetic effect prevails, this region being characterized by FM and AF correlations of comparable amplitude. While one can only speculate on the fact that we do not find an AF ground state, guessing that it is a finite-size effect, the reason why we find no FM order is that the conditions under which Nagaoka's theorem holds are never satisfied. Indeed there is no parameter regime where the phononic renormalization yields $U^* \gg t^*$, with t^* remaining at the same time finite.

D. $N=4$, half-filled case

In Fig. 9 we report the phase diagram at half-filling for $\Gamma=1$ Å^{-1}, both with and without the phonon-induced next-nearest-neighbor interaction. For intermediate to large a we see that an antiferromagnetic phase is stable for small $g^2/\hbar\Omega$ while a charge ordered state of 2-0-2-0 type is stable for large $g^2/\hbar\Omega$. For small a and irrespective of $g^2/\hbar\Omega$, a nonmagnetic ground state characterized by the absence of any spin correlations is found to be stable, wedging in between the AF and CO regions at small $g^2/\hbar\Omega$ up to $a\sim 2.5$ Å.

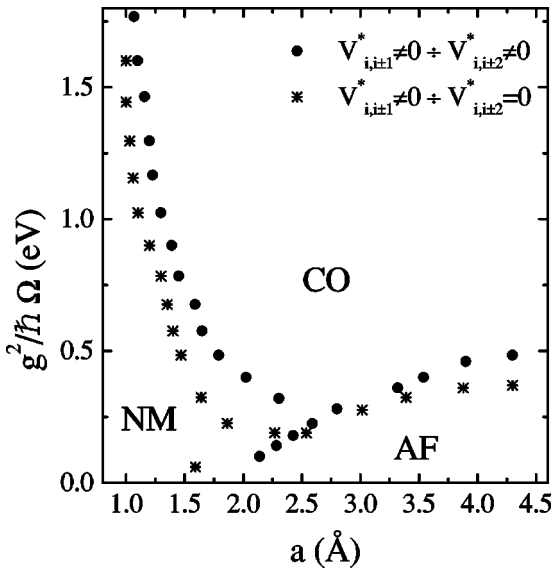

FIG. 9. Phase diagram for $N=4$ and $\Gamma=1$ Å^{-1}. The regions labeled NM, CO, and AF are characterized by vanishing magnetization, charge order, and antiferromagnetism, respectively.

We can also see that taking into account the effect of $V^*_{i,i\pm2}$ leads to quantitatively significant modifications of the phase diagram. Indeed, even if the negative value of $V^*_{i,i\pm2}$ is rather small for low $g^2/\hbar\Omega$ values, it causes an appreciable expansion of the NM region toward higher $g^2/\hbar\Omega$ and a values, with a corresponding reduction of the CO and AF regions, due to the fact that for increasing $g^2/\hbar\Omega$ (or a) $V^*_{i,i\pm2}$ becomes negative, and thus opposite in sign to $V^*_{i,i\pm1}$.

Let us now discuss how the system responds as the value of a is increased, for $g^2/\hbar\Omega=0.1$ eV. As shown in Fig. 9, the system passes from the NM regime to the AF regime. The position and nature of this transition can be easily identified by looking at the behavior of the correlation functions plotted in Fig. 10.

For a lower than $\simeq 2.2$ Å, χ^s_n and χ^s_{nn} are close to zero and almost coinciding, which corresponds to a regime without significant magnetic correlations. On the other hand, for higher values of a one has $\chi^s_n \approx -0.5$, which corresponds to an antiparallel configuration of spins on first neighbors, and $\chi^s_{nn}\approx 1/4$, which indicates a configuration of parallel spins on next-nearest neighbors. This behavior of χ^s_n and χ^s_{nn} clearly shows that the ground state has antiferromagnetic correlations. The middle panel of Fig. 10 gives indications on the charge distribution. In the NM region we can see that even though the site occupation is still fluctuating because of the itinerancy of the carriers, nonetheless there is some precursor of the CO phase, as a consequence of the fact that the values of χ^c_{nn} are considerably higher than those of χ^c_n. Conversely, in the AF region χ^c_n and χ^c_{nn} become constant and equal to 1, thus indicating that there is one electron per site on the average.

The same qualitative trend is found in the charge-deformation CF's, shown in the bottom panel of Fig. 10. At small a the charge-related deformation also appreciably affects first- and second-neighbor sites. Then, as the NM-AF

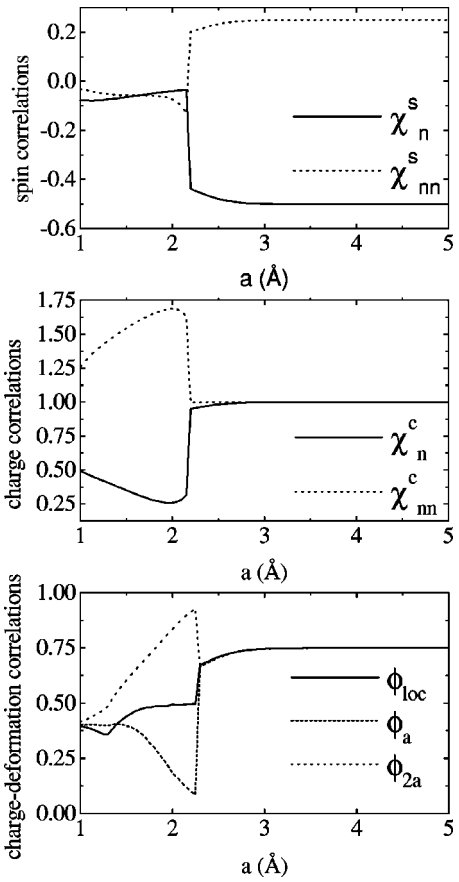

FIG. 10. Spin (top panel), charge (middle panel), and charge-deformation (bottom panel) correlation functions for $N=4$ at $g^2/\hbar\Omega=0.1$ eV.

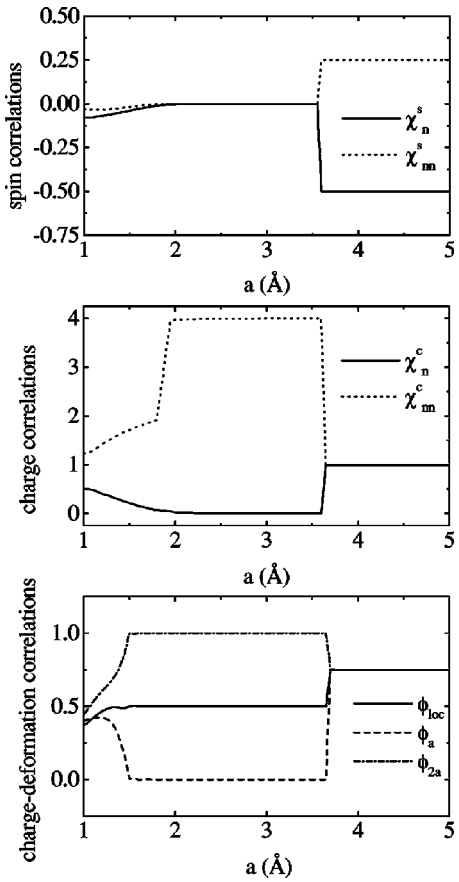

FIG. 11. Spin (top panel), charge (middle panel), and charge-deformation (bottom panel) correlation functions for $N=4$ at $g^2/\hbar\Omega=0.4$ eV.

boundary is approached, Φ_{loc} tends to stay constant, while Φ_{2a} grows considerably and Φ_a becomes small, resulting in a behavior that can be considered as a precursor of the CO state. When the AF state sets in, all three charge-deformation CF's come to coincide at a rather large value, indicating that, in a regular pattern of site occupancy, all orders of neighbors are equally affected. In terms of the size of the polarons, one can say that for $N=4$ they tend to show an extended character, i.e., the associated deformation develops beyond the site where the charge is located.

The behavior of the renormalized electronic parameters (not shown) is such that in the AF region t^* is vanishingly small, driving the system in a regime of electron localization where the mechanism of superexchange dominates. Conversely, in the NM region, the hopping term is only weakly renormalized, because the localization effect due to the displacement is counteracted by the squeezing, so that the electrons are rather mobile. Moreover, U^* and $V^*_{i,i\pm1}$ are comparable in magnitude, thus preventing the formation of local pairs as well as of long-range ordering. In terms of an equivalent t-J model, the NM ground state does not show any well-defined spin or charge order since t^* remains large enough to have two concurrent effects: on the one hand, it opposes a complete charge disproportionation, and, on the other hand, it gives rise to a kinetic exchange proportional to $2t^{*2}/(U^*-V^*_{i\pm1})$, strong enough to allow for some magnetic coupling effects. As in the previous cases, the energy difference between the NM and AF states is small enough for the tiny negative value of $V^*_{i,i\pm2}$ to have a sizable effect on the position of the phase boundaries.

When $g^2/\hbar\Omega=0.4$ eV, a reentrant behavior can be deduced from the phase diagram in Fig. 9 as a is increased. This is made evident by the behavior of the correlation functions in Fig. 11. For a between approximately 2 Å and 3.6 Å, χ^c_n is equal to zero (middle panel), while χ^c_{nn} assumes the largest value (~ 4), clearly indicating a CO configuration of alternating empty and doubly occupied sites. As expected, in this same range of a the spin correlation functions (upper panel) are zero since configurations, with zero and two electrons on each site prevent the formation of magnetic moments. As far as the charge-deformation CF's are concerned, we see that in the charge-density-wave (CDW) region the largest values are taken by Φ_{2a}, with the nearest-neighbor CF Φ_a always remaining very small, and the on-site CF Φ_{loc} taking values which are intermediate between Φ_{2a} and Φ_{loc}. This can clearly be considered as a further evidence of the formation of a CO state of the 2-0-2-0 type. When a lies out of this intermediate range, the correlation functions behave essentially as in the case $g^2/\hbar\Omega=0.1$ eV.

The renormalized electronic parameters (not shown) fully support this picture. In the CDW region the electron mobility is equal to zero, $V^*_{i,i\pm2}$ is attractive, and $V^*_{i,i\pm1}$ is repulsive

and comparable in magnitude to U^*. This evidently tends to promote configurations with alternating empty and doubly occupied sites. To the extent that the effects of including V_{ij}^* can be neglected, our results qualitatively agree with other studies.[3]

We end this section by noting that discontinuities in the correlation functions and the renormalized parameters, seen in the above figures, should not be interpreted as a signature of a real first-order localization transition. Rather they are a consequence of a drawback affecting all variational methods, which, as is well known, can only provide an upper bound to the true ground-state energy. This leads to a violation of the exact results demonstrated by Löwen,[33] according to which the self-trapping transition generated by an interacting term of the Holstein type is an analytical crossover for any value of the electron-phonon coupling, and not an abrupt (nonanalytical) phase transition.

IV. CONCLUSIONS

The method that we have used to obtain an effective polaronic Hamiltonian from the generalized Holstein-Hubbard Hamiltonian, based on the use of displacement and squeezing transformations, while allowing technically simple calculations, still permits us to grasp some basic physical effects, such as, for instance, the phonon-induced renormalization of the electronic interaction parameters. In this respect, this approach might be of interest, for instance, in the theoretical analysis of high-T_c superconductivity, where it can provide clues to select among electron-phonon models or purely electronic models. If, in the comparison between theory and experiments, one refers to phonon-renormalized, and not bare, interactions, then even phenomena such as the isotope effect could find an explanation within the framework of a model with only electronic degrees of freedom. An improvement of the approach followed here may be obtained by suitably dealing with two limitations, that is, (i) the factorization of the fermion-boson wave function into separate fermionic and bosonic factors, and (ii) the use of a squeezed phonon wave function (whose intrinsic limitations have been discussed in Ref. 14) for the elimination of the phononic degrees of freedom. Further studies in this direction are planned for the near future.

The results we have presented support our claim that, in working out an effective Hamiltonian through displacement and squeezing transformations, it is important to take into account the momentum dependence of the displacement and squeezing parameters, to avoid losing a significant part of the physical content of the model. We have indeed shown that the effective phonon-induced intersite charge interaction that one obtains[24,25] by going beyond the LFA should be carefully taken into account, as it has appreciable effects on the phase diagram, particularly for $N=4$ and 2. This latter case is particularly significant, because theoretical studies[4,34] of the occurrence of doping-induced inhomogeneities in the charge distribution in both colossal magnetoresistance manganites and superconducting cuprates point to the importance of the long-range charge interaction, but have difficulties in justifying its presence in metallic systems, where it should vanish beyond a very short distance due to the screening induced by the itinerant carriers. Differently from the purely electronic V_{ij}, the effective V_{ij}^* can be seen as an independent parameter providing the needed long-range interaction through a mechanism depending basically on the phonons, and only weakly on the doping. In real systems such as the superconducting cuprates, this mechanism can be ascribed to the Holstein-type electron-phonon coupling generated by the ion dynamics out of the conducting layers. Additionally, $V_{i,i\pm 2}^*$ can vary both in amplitude and, most importantly, in sign, depending on the phononic state and on the value of the lattice constant.

From a more general point of view, our results show that there exist, for $N=2$ and 3, regions of the phase diagram where the ground state of a hole-doped correlated system with strong electron-phonon interaction, on the one hand, has appreciable coexisting spin and charge correlations, while, on the other hand, is such that the carriers retain their itinerancy to a large extent. This suggests that the debate on whether charge or spin fluctuations in the normal state are responsible for high-temperature superconductivity might be viewed from a different perspective, namely, by considering that, under appropriate conditions, both fluctuations can coexist, possibly cooperating to build the superconductive phase.

A significant result is that, for $N\geqslant 2$, in the disordered regions of the phase diagrams for low values of a and $g^2/\hbar\Omega$, we find wide subregions characterized by strong precursory charge-ordering effects, whose amplitude can change very rapidly with the lattice parameter. The effect is particularly evident in the case $N=2$. This might be of interest with respect to the recently reported[27] microscopically coexisting charge and structural dishomogeneities in underdoped and optimally doped $La_{2-x}Sr_xCuO_4$ samples.

Finally, we have been able to model the effects of a varying lattice spacing. This might be of relevance in all cases in which compression (or expansion) of the lattice causes sharp phase transitions. In particular, our results show that in the range of a where a given state is stable, even if that state does not show a fully developed symmetry-breaking order parameter (CO or AF), still the behavior of some correlation functions may be characterized by drastic changes as the site distance is varied.

ACKNOWLEDGMENTS

Interesting discussions with R. Iglesias, M. A. Gusmão, A. Painelli, and H. Zheng are gratefully acknowledged.

[1] J. Ranninger, Phys. Rev. B **48**, 13 166 (1993); S. Sil, J. Phys.: Condens. Matter **11**, 8879 (1999).
[2] M. Deeg, H. Fehske, and H. Büttner, Z. Phys. B: Condens. Matter **91**, 31 (1993).
[3] U. Trapper, H. Fehske, M. Deeg, and H. Büttner, Z. Phys. B: Condens. Matter **93**, 465 (1994); H. Fehske, D. Ihle, J. Loos, U. Trapper, and H. Büttner, *ibid.* **94**, 91 (1994).
[4] F. Becca, M. Tarquini, M. Grilli, and C. Di Castro, Phys. Rev. B **54**, 12 443 (1996).
[5] A. La Magna and R. Pucci, Phys. Rev. B **55**, 14 886 (1997).
[6] K. Yonemitsu, J. Zhong, and H.-B. Schüttler, Phys. Rev. B **59**, 1444 (1999).
[7] V. Cataudella, G. De Filippis, and G. Iadonisi, Phys. Rev. B **60**, 15 163 (1999).
[8] J. Bonča, T. Katrašnik, and S.A. Trugman, Phys. Rev. Lett. **84**, 3153 (2000).
[9] H. Zheng, Phys. Rev. B **36**, 8736 (1987); Phys. Lett. A **131**, 115 (1988); D.L. Lin and H. Zheng, J. Appl. Phys. **64**, 5905 (1988); H. Zheng, J. Phys.: Condens. Matter **1**, 1641 (1989); H. Zheng, D. Feinberg, and M. Avignon, Phys. Rev. B **41**, 11 557 (1990); H. Zheng, Z. Phys. B: Condens. Matter **82**, 363 (1991).
[10] J. Takimoto and Y. Toyozawa, J. Phys. Soc. Jpn. **52**, 4331 (1983); W. Schmidt and M. Schreiber, J. Chem. Phys. **86**, 953 (1987); J. Ranninger and U. Thibblin, Phys. Rev. B **45**, 7730 (1992); J. Ranninger, Solid State Commun. **85**, 929 (1993); M. Capone, W. Stephan, and M. Grilli, Phys. Rev. B **56**, 4484 (1997); T. Hotta and Y. Takada, Physica B **230-232**, 1037 (1997); E.V.L. de Mello and J. Ranninger, Phys. Rev. B **58**, 9098 (1998).
[11] H. Fehske, H. Röder, G. Wellein, and A. Mistriotis, Phys. Rev. B **51**, 16 582 (1995).
[12] F. Marsiglio, Physica C **244**, 21 (1995).
[13] G. Wellein, H. Röder, and H. Fehske, Phys. Rev. B **53**, 9666 (1996).
[14] G.-P. Borghi, A. Girlando, A. Painelli, and J. Voit, Europhys. Lett. **34**, 127 (1996).
[15] H. Fehske, G. Wellein, B. Bäuml, and H. Büttner, Physica B **230-232**, 899 (1997).
[16] M. Acquarone, J.R. Iglesias, M.A. Gusmão, C. Noce, and A. Romano, J. Supercond. **10**, 305 (1997); Phys. Rev. B **58**, 7626 (1998). Note that V in Eq. (1) here corresponds to $V-J/2$ in the last paper, due to a misprint in Eq. (1) there.
[17] C. Zhang, E. Jeckelmann, and S.R. White, Phys. Rev. B **60**, 14 092 (1999).
[18] M. Wagner, *Unitary Transformations in Solid State Physics* (North-Holland, Amsterdam, 1986).
[19] W.-M. Zhang, D.-H. Feng, and R. Gilmore, Rev. Mod. Phys. **62**, 867 (1990); R. Muñoz-Tapia, Am. J. Phys. **61**, 11 (1993).
[20] X. Wang and H. Zheng, Phys. Rev. B **52**, 15 261 (1995).
[21] H. Zheng and S.Y. Zhu, Phys. Rev. B **55**, 3803 (1997); H. Zheng and M. Avignon, *ibid.* **58**, 3704 (1998).
[22] I.G. Lang and Y.A. Firsov, Zh. Éksp. Teor. Fiz. **43**, 1843 (1962) [Sov. Phys. JETP **16**, 1301 (1963)].
[23] D. Emin, Phys. Rev. B **39**, 6575 (1989); J. Coste and J. Peyraud, Z. Phys. B: Condens. Matter **96**, 185 (1994).
[24] M. Acquarone, Acta Phys. Pol. B **29**, 3591 (1998).
[25] A. Alexandrov and J. Ranninger, Phys. Rev. B **23**, 1796 (1981).
[26] A. Bianconi, N.L. Saini, T. Rossetti, A. Lanzara, A. Perali, M. Missori, H. Oyanagi, H. Yamaguchi, Y. Nishihara, and D.H. Ha, Phys. Rev. B **54**, 12 018 (1996); A. Lanzara, N.L. Saini, A. Bianconi, J.L. Hazemann, Y. Soldo, F.C. Chou, and D.C. Johnston, *ibid.* **55**, 9120 (1997); J.M. Tranquada, J. Phys. Chem. Solids **59**, 2150 (1998); S. Mori, C. H. Chen, and S. W. Cheong, Nature (London) **392**, 473 (1998); C.N.R. Rao, R. Mahesh, A. K. Raychaudhuri, and R. Mahendiran, J. Phys. Chem. Solids **59**, 487 (1998).
[27] E.S. Božin, G.H. Kwei, H. Takagi, and S.J.L. Billinge, Phys. Rev. Lett. **84**, 5856 (2000).
[28] H. Zheng, Phys. Rev. B **38**, 11 685 (1988).
[29] C. Noce and M. Cuoco, Phys. Rev. B **56**, 13 047 (1996).
[30] M. Acquarone, M. Cuoco, and C. Noce, Int. J. Mod. Phys. B **13**, 1183 (1999); M. Acquarone, M. Cuoco, C. Noce, and A. Romano, Physica B **284-288**, 1561 (2000).
[31] A.S. Alexandrov, Phys. Rev. B **61**, 12 315 (2000).
[32] L.F. Feiner, J.H. Jefferson, and R. Raimondi, Phys. Rev. B **53**, 8751 (1996).
[33] H. Löwen, Z. Phys. B: Condens. Matter **71**, 219 (1988); Phys. Rev. B **37**, 8661 (1988); B. Gerlach and H. Löwen, Rev. Mod. Phys. **63**, 63 (1991).
[34] G. Seibold, C. Castellani, C. Di Castro, and M. Grilli, Phys. Rev. B **58**, 13 506 (1998); A. Sadori and M. Grilli, Phys. Rev. Lett. **84**, 5375 (2000).
[35] J. Spalek and W. Wojcik, Phys. Rev. B **45**, 3799 (1992); J. Spalek, R. Podsiadly, W. Wojcik, and A. Rycerz, Phys. Rev. B **61**, 15 676 (2000).